Check for updates

High ANO1 expression is a prognostic factor and correlated with an immunosuppressive tumor microenvironment in pancreatic cancer

Guangnian Zhang[1†], Zhihui Shu[1†], Jun Yu[1], Jianshui Li[1], Pengsheng Yi[1], Bin Wu[1], Dawei Deng[1], Shu Yan[1], Yong Li[1], Dongmei Ren[1], Yifu Hou[2,3]* and Chuan Lan[1]*

[1]Department of Hepatobiliary Surgery and Center of Severe Acute Pancreatitis, The Affiliated Hospital of North Sichuan Medical College, Nanchong, China, [2]Department of Organ Transplantation, Sichuan Provincial People's Hospital, University of Electronic Science and Technology of China, Chengdu, China, [3]Clinical Immunology Translational Medicine Key Laboratory of Sichuan Province & Organ Transplantation Center, Sichuan Provincial People's Hospital, University of Electronic Science and Technology of China, Chengdu, China

Background: Aminooctylamine (ANO1) plays an oncogenic role in various cancers. However. its role in pancreatic cancer (PC) has rarely been studied. This study investigated the prognostic value of ANO1 and its correlation with the tumor microenvironment (TME) in PC.

Methods: Consecutive patients with PC (n = 119) were enrolled. The expression of ANO1 in cancer cells, the expression of fibroblast activation protein (FAP) and alpha smooth muscle actin in cancer-associated fibroblasts (CAFs), and the numbers of CD8- and FOXP3-positive tumor-infiltrating lymphocytes (TILs) were evaluated using immunohistochemistry. The prognostic value of ANO1 and its correlation with CAF subgroups and TILs were analyzed. The possible mechanism of ANO1 in the TME of PC was predicted using the the Cancer Genome Atlas (TCGA) dataset.

Results: The expression of AN01 was correlated with overall survival (OS) and disease-free survival. Multi-factor analysis showed that high ANO1 expression was an independent adverse prognostic factor for OS (hazard ratio, 4.137; P = 0.001). ANO1 expression was positively correlated with the expression of FAP in CAFs (P < 0.001) and negatively correlated with the number of CD8-positive TILs (P = 0.005), which was also validated by bioinformatics analysis in the TCGA dataset. Moreover, bioinformatic analysis of the TCGA dataset revealed that ANO1 may induce an immunosuppressive tumor microenvironment in pancreatic cancer in a paracrine manner.

Conclusion: ANO1 is a prognostic factor in patients with PC after radical resection. ANO1 may induce an immunosuppressive tumor microenvironment in PC in a paracrine manner, suggesting that ANO1 may be a novel therapeutic target.

1 Introduction

Pancreatic cancer (PC) ranks the third leading cause of cancer-related death in the developed countries and is expected to be the second-leading cause of cancer-related mortality by 2040 (1, 2). Interest in PC has increased owing to its increasing annual incidence and high mortality (3). Currently, surgery is the main curative treatment for patients with PC. However, less than 20% of patients are suitable for operation at diagnosis (4). Furthermore, even in cases where surgery is suitable, about 75% of them will experience recurrence within 2 years (5), and the 5-year overall survival (OS) rate remains only less than 10% (6). For patients with recurrent or advanced tumors, other treatments, including chemotherapy, radiotherapy, and immune therapies, have shown limited efficacy. Therefore, it is necessary to determine and implement the new treatment strategies that benefit more patients.

Aminooctylamine (ANO1) is a calcium-activated chloride channel protein (7) which serves the functions such as smooth muscle contraction, the epithelial ion transport and glandular secretion (8, 9). In studies to date that have shown that ANO1 is overexpressed in multiple diseases and tumor types and contributes to the process of carcinogenesis (10). For example, in esophageal squamous cell carcinoma, both mRNA and protein levels of ANO1 were upregulated and correlated with an unfavorable clinical prognosis (11). Additionally, ANO1 is highly expressed in breast, ovarian, and hepatocellular carcinomas and promotes the malignant biological behavior of cancer cells (12–14). Although one research showed that ANO1 was overexpressed in PC (15), the prognostic value and specific role of ANO1 in PC progression remain unclear, and its association with the tumor microenvironment (TME) has not been explored.

TME play a crucial role in regulating cancer cells progression. This topic has received increasing appreciation recently. The pancreatic TME contains multiple fibroblasts and heterogeneous immune cell populations with inhibitory effects (16). Cancer-associated fibroblasts (CAFs) are a heterogeneous group consisting of myofibroblast CAFs (myCAFs), inflammatory CAFs (iCAFs), and antigen-presenting CAFs (17). MyCAFs are located near tumor cells and is considered to be the cause of the extracellular matrix deposition. iCAFs tend to dominate the space between islands of PC cells and release inflammatory cytokines such as interleukin-6 (IL-6) (18). Fibroblast activation protein (FAP) and alpha smooth muscle actin (α-SMA) are markers of myCAFs and iCAFs, respectively. Recent studies have shown that targeted FAP-positive CAFs may inhibit tumor growth (19–21). In addition, the absence of FAP in the stromal cells delayed the progression of PC disease in mice (19). α-SMA-positive CAFs have tumor-inhibiting effects in a genetically engineered mouse model of PC and contribute to the differentiate of tumor-infiltrating T cells (22). Positive α-SMA was associated with increased OS, whereas positive FAP was associated with decreased OS (23). Tumor-infiltrating lymphocytes (TILs) represent the immune response to tumor progression, and they are another important component of TME (24). CD8 and FOXP3 play important but opposite roles in cancer and are two specific subgroups of TILs (21). CD8-positive TILs are key immune cells in tumor immunity that kill cancer cells by triggering apoptosis, while foxp3 positive TILs are regulatory T cells (Tregs) with immunosuppressive functions that inhibit the proliferation and activation of CD8-positive TILs (25). A recent study found that IL-6 secreted by α-SMA positive CAF conferred chemotherapy resistance and negatively regulated T cells in the TME (26). In addition, growth factors and inflammatory cytokines secreted by CAFs activate oncogenic pathways in cancer cells. Interestingly, IL-6 and epidermal growth factor promote the expression of ANO1 by signal transducer and transcriptional activator 3 and phosphatidylinositol 3 kinase/protein kinase B signaling (27). This suggests that ANO1 levels can be regulated in cancer cells by cytokines, which may be the molecular mechanism by which ANO1 is involved in inflammation and tumor immunity. However, whether ANO1 regulates TIL and CAF populations in PC is unclear and requires further investigation.

Therefore, the aims of this study were to probe into the prognostic value of ANO1 in PC patients and explore the relationship between ANO1 expression and TIL and CAF populations.

Abbreviations: ANO1, aminooctylamine; CAF, cancer-associated fibroblast; DFS, disease-free survival; FAP, fibroblast activation protein; FOXP3, forkhead box protein 3; iCAF, inflammatory cancer-associated fibroblast; IL-6, Interleukin-6; myCAF, myofibroblast cancer-associated fibroblast; OS, overall survival; PC, pancreatic cancer; ssGSEA, single sample gene set enrichment analysis; TIL, tumor-infiltrating lymphocytes; TME, tumor microenvironment; Treg, regulatory T cell; α-SMA, alpha smooth muscle actin.

2 Materials and methods

2.1 Patients and specimens

A total of 119 patients with pathologically confirmed PC who underwent surgery in the Affiliated Hospital of North Sichuan Medical College from January 2016 to June 2022 were included in this single-center study. None of the participants had received radiotherapy or chemotherapy before surgery, and their clinical data were complete. Fluorouracil or gemcitabine are mainly used as adjuvant chemotherapy. The pathological classification of pancreatic cancer was based on the 2019 WHO classification, and TNM staging is based on the American Joint Committee on Cancer 8th edition of the cancer staging system.

Clinical examinations and enhanced computed tomography were performed at 3-month intervals after the initial surgery for primary PC. Disease-free survival (DFS) was defined as the time from surgery to tumor recurrence or death. OS was defined as the time from surgery to death.

Written informed consent was obtained from all the patients, and the research program was approved by the Institutional Review Committee of the Affiliated Hospital of North Sichuan Medical College (number: 2023ER041-1). We adhered to the ethical standards of the relevant local and national human experimentation committees, as well as the 1964 Declaration of Helsinki and its subsequent amendments.

2.2 Immunohistochemistry and evaluation of TILs and CAFs

Paraffin-embedded sliced of PC patients were dewaxed in xylenes and ethanol and autoclaved in the fluid of the antigen repair (MVS-0100; Maixin biotechnology; Fuzhou; China) for 15 min to repair epitope of antigen. Immunohistochemical staining was performed using a ready-to-use immunohistochemical UltraSensitive SP reagent (mouse/rabbit) (KIT-9710; Maixin biotechnology; Fuzhou; China). Endogenous peroxidase activity was interdicted using an endogenous peroxidase blocker (reagent 1) for 10 min at room temperature and a non-specific stain blocker (reagent 2) for 10 minutes at room temperature. For CD8 and FOXP3 dyeing, we adopt rabbit polyclonal anti-CD8 (1:200 dilution; AF5126; Affinity Biosciences; Jiangsu; China) and anti-FOXP3 (1:200 dilution; AF6544; Affinity Biosciences; Jiangsu; China) antibodies, respectively. For FAP and α-SMA staining, we adopt anti-FAP (1:50 dilution; AF5344; Affinity Biosciences; Jiangsu; China) and anti-α-SMA (1:100 dilution; AF1032; Affinity Biosciences; Jiangsu; China) antibodies, respectively. Section of tissue were incubated with the primary antibody at 4°C overnight. They were then incubated with biotin-labeled sheep anti-mouse/rabbit IgG polymer (reagent 3) for 10 min at room temperature, Streptomyces anti-biotin protein-peroxidase (reagent 4) for 10 min at room temperature, and DAB (DAB-0031; Maixin biotechnology; Fuzhou; China) solution for color development for 1-3 min. Slides

were then counterstained with hematoxylin. Two researchers ignored the clinicopathological data and evaluated the stained slides using a ×200 light microscope. For CD8 and FOXP3 staining, sequential slices of tumor sections of each patient was evaluated. The number of positive cells in a field 1 mm in diameter were counted in three fields containing a large number of cancer cells, and the results were expressed as the average of the counts in triplicate (number of cells per field). The one-way scoring system based on the dyeing strength of FAP and alpha SMA in CAFs expression for immunohistochemical analysis. The intensity of staining was divided into 0(no staining), 1(weak staining), 2 (moderate staining), and 3(strong staining). Intensity of Staining of 0 or 1 was defined as the negative expression of FAP and α-SMA in CAFs, and staining intensity of 2 or 3 was defined as positive expression of FAP and α-SMA in CAFs.

2.3 Immunohistochemistry and evaluation of ANO1 positivity

Sample handling and immunohistochemistry were performed as mentioned above. After blocking endogenous peroxidase activity, samples were incubated with diluted ANO1 antibody (1:100 dilution; DF7769; Affinity Biosciences; Jiangsu; China) overnight, and assays were performed using reagents 3 and 4. A DAB color solution was used to observe a positive reaction, and slides were counterstained with hematoxylin. All staining results were scored independently by two researchers ignored the clinicopathological data as described above. Intensity of staining was rated to negative, weak, moderate, and strong expression, respectively. Negative or weak ANO1 expression was regarded as negative staining, and moderate or strong ANO1 expression was regarded as positive staining.

2.4 Bioinformatics and survival analyses

GEPIA was used to obtain the OS and DFS survival plots of ANO1 from the TCGA dataset. We used 50% as a cutoff value. A log-rank test was used to assess difference in survival between patients with high and low ANO1 expression. Hazard ratios and p-values were calculated using univariate Cox regression analysis.

2.5 Single sample gene set enrichment analysis and calculation of the ImmuneScore and StromalScore

Tumor-infiltrating immune cells were quantified by ssGSEA using the GSVA package in R. ssGSEA applies the gene signatures expressed by immune cell populations to individual cancer samples. The deconvolution approach used in this study included CD8-positive T cells and Tregs. We used the ssGSEA algorithm to explore the relationship between ANO1 expression and the

infiltration of CD8-positive T cells and Tregs based on the PC dataset in TCGA (Firehose Legacy). The correlation between ANO1 and tumor-infiltrating immune cells was assessed using Spearman's test.

After selecting the samples, we extracted the expression matrix from the samples and calculated the immune purity of the expression matrix using the "estimate" R package. We performed ssGSEA for each sample, and the immune infiltration (ImmuneScore) and overall stromal content (StromalScore) were calculated using the ESTIMATE algorithm.

2.6 Selection of differentially expressed genes

The patients were divided into high- and low-score groups based on the cutoff value of 50%. The selection of DEGs was performed according to the published method using the "edgeR" R package with P <0.05 and |logFC| >1. A volcano plot was used to visualize the DEGs. Network enrichment analysis was performed using gene set enrichment analysis (http://software.broadinstitute.org/gsea/index.jsp) to identify the possible pathways affected by ANO1. Moreover, a heatmap was generated to describe the upregulated or downregulated intersection genes of DEGs in pathways using a website tool (http://bioinformatics.psb.ugent.be/webtools/Venn/).

2.7 Statistical analyses

Continuous variables that conformed to a normal distribution are represented by the mean ± standard deviation, and continuous variables that did not conform to a normal distribution are represented by the median (upper quartile-lower quartile). The significance of differences was assessed using Student's t-test or the Mann-Whitney U test. Differences in categorical variables were evaluated using the chi-squared test or Fisher's exact test, as appropriate. Predictors of prognosis were determined using Cox proportional hazards regression analysis. Clinicopathological factors were analyzed by multivariable analysis, which included variables with P < 0.05 in the univariate analysis. The Kaplan–Meier method was used to estimate OS and DFS, and the log-rank test was used to compare survival curves. The Wilcoxon rank sum test and chi-square test were used for correlation analysis. P < 0.05 was considered statistically significant. All tests were performed using IBM SPSS Statistics 19 software.

3 Results

3.1 Patient characteristics

There were about 119 patients with PC who underwent surgical resection in all were enrolled in this study Among them, 73 (61.3%) experienced tumor recurrence and 90 (75.6%) died. The median follow-up period was 37 months.

We assessed the expression of ANO1 in tissue samples from PC patients; 74 patients had positive ANO1 expression and 45 had negative ANO1 expression (Figure 1A). FAP and α-SMA expression in the CAFs was also assessed (Figures 1B, C). There were 74 patients with FAP positivity and 45 with FAP negativity, whereas there were 57 patients with α-SMA positivity and 62 with α-SMA negativity. CD8-positive TILs and FOXP3-positive TILs were also counted, and patients were defined as having high or low expression according to the 50% cutoff value (Figures 1D, E).

3.2 ANO1 expression was an independent prognostic factor for patients with pancreatic cancer

Table 1 sum up the clinicopathological features of the ANO1-positive and ANO1-negative groups. There were no obvious differences in age, sex, total bilirubin level, CA19-9 level, tumor size, tumor differentiation, pT, pN, nerve invasion, and tumor location between ano1 positive and ano1 negative groups.

When using the immunohistochemistry results, Kaplan–Meier analysis showed that positive ANO1 expression was meaningfully associated with poor OS (log rank P < 0.001) and poor DFS (log rank P < 0.001) (Figure 2A). Similarly, in the TCGA dataset, high ANO1 mRNA levels were correlated with poor OS and DFS (Figure 2B).

Univariate and multivariate Cox regression analyses displayed that lymphatic metastasis (hazard ratio = 4.073, P = 0.001) and ANO1 expression (hazard ratio = 4.137, P = 0.001) were independent risk factors of the OS (Table 2).

3.3 The relationships between ANO1 expression and CAF subgroups

Kaplan–Meier analysis showed that positive FAP expression in CAFs was expressively associated with poor OS (log rank P = 0.002) and poor DFS (log rank P = 0.009), indicating that FAP-positive CAFs are associated with poor prognosis (Figure 3A). ANO1 expression was really correlated with FAP expression in CAFs (P < 0.001); however, ANO1 expression and α-SMA expression in CAFs had no virtual correlation (P = 0.179) (Figure 3B).

3.4 The relationship between ANO1 expression and TILs

ssGSEA was performed to probe into the correlation between ANO1 expression and immune cell infiltration. The expression of ANO1 was inversely associated with the infiltration of CD8-positive TILs (P < 0.01) and had a potential relevance to FOXP3-positive TILs without a significant difference (Figure 4A). Interestingly, our IHC results were similar. ANO1 expression was inversely correlated
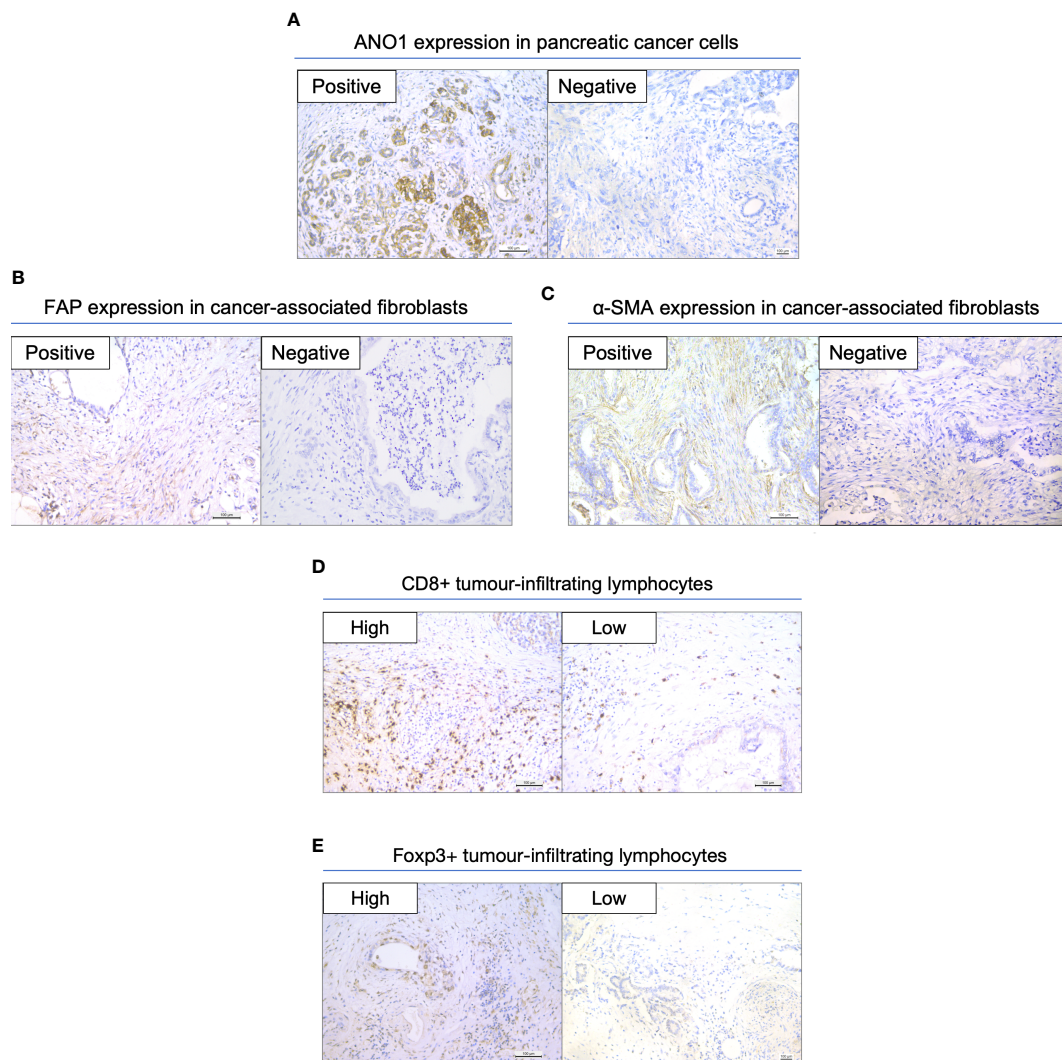
FIGURE 1

Immunohistochemical staining in resected pancreatic cancer specimens. **(A)** Expression of ANO1 in cancer cells. **(B)** Expression of FAP in CAFs. **(C)** Expression of α-SMA in CAFs. **(D)** Expression of CD8 in TILs. **(E)** Expression of FOXP3 in TILs. Scale bar = 100 μm. ANO1, aminooctylamine; FAP, fibroblast activation protein; CAF, cancer-associated fibroblast; α-SMA, alpha smooth muscle actin; TIL, tumor-infiltrating lymphocyte; FOXP3, forkhead box protein 3.

with CD8-positive TILs (P = 0.005) and possibly positively correlated with FOXP3-positive TILs (Figure 4B).

3.5 ANO1 may induce an immunosuppressive tumor microenvironment in pancreatic cancer through a paracrine manner

These results indicate that ANO1 may be highly correlated with an immunosuppressive tumor microenvironment in PC by interacting with FAP-positive CAFs and CD8-positive TILs. To further assess this, immune inFIltration (ImmuneScore) and total stromal content (StromalScore) were calculated using the ESTIMATE algorithm, and the results revealed that high ANO1 expression was correlated with a relative higher StromalScore and lower ImmuneScore (Figure 5A).

Bioinformatics analysis of the TCGA dataset was used to explore how ANO1 induces an immunosuppressive tumor microenvironment. We used the cutoff value that induced the most valid difference as the expression threshold to class the high and low ANO1 expression cohorts. In total, 890 genes were upward and 3355 genes were downward (Figure 5B). Furthermore, Reactome pathway enrichment analysis showed that "cytokine signaling in immune system" and "signaling by interleukins" were two possible pathways associated with ANO1, and KEGG pathway enrichment break down revealed that "cytokine-cytokine receptor interaction" was a possible pathway associated with ANO1 (Figure 5C). A heat map and Table 3 showed that multiple cytokines and receptors were highly correlated with ANO1

TABLE 1 Clinicopathological features based on ANO1 expression.

Characteristic	Total (n = 119)	ANO1 expression		p value
		Negative (n = 45)	Positive (n = 74)	
Age (y)	64.2 ± 9.4	63.6 ± 8.3	64.5 ± 10.1	0.449
Sex				0.550
Male	78 (65.5%)	31 (68.9%)	47 (63.5%)	
Female	41 (34.5%)	14 (31.1%)	27 (36.5%)	
CA19-9 (ng/mL)	216.9 (48.9-860.2)	182.8 (47.7-883.6)	227.5 (50.7-908.8)	0.485
Total bilirubin(μmol/L)	46.0 (19.1-174.7)	31.2 (18.9-165.3)	67.3 (19.5-198.0)	0.734
Tumor size (mm)	30 (20-40)	30 (20-40)	28 (20-40)	0.402
pT				0.286
T1/2	81 (68.1%)	28 (62.2%)	53 (71.6%)	
T3/4	38 (38.9%)	17 (37.8%)	21 (28.4%)	
pN				0.987
N0	66 (55.5%)	25 (55.6%)	41 (55.4%)	
N1	53 (44.5%)	20 (44.4%)	33 (44.6%)	
Differentiation				0.141
Well/Moderate	76 (63.9%)	25 (55.6%)	51 (68.9%)	
Poor	43 (36.1%)	20 (44.4%)	23 (31.1%)	
Nerve invasion				0.321
ne0	41 (34.5%)	18 (40%)	23 (31.1%)	
ne1,2,3	78 (65.5%)	27 (60%)	51 (68.9%)	
Location				0.236
Head	69 (58.0%)	23 (51.1%)	46 (62.2%)	
Neck, body, and tail	50 (42.0%)	22 (48.9%)	28 (37.8%)	

Data are presented as mean ± standard deviation, n (%), or median (25-75%).
CA19-9, Carbohydrate antigen-199.

expression (Figure 5D). In summary, the function of ANO1 in the TME may involve paracrine mechanisms.

4 Discussion

Multiple studies have identified the effects of ANO1 on tumor cells in various types of cancer,however, its effects on PC and the TME of PC have rarely been studied. Our results indicate that ANO1 positivity is an independent risk factor for PC. Further, ANO1 expression correlated positively with accumulation of FAP-positive CAFs. ANO1 high expression was significantly correlated with a lower number of CD8-positive TILs and possibly correlated with a high number of FOXP3-positive TILs. Because increased FAP-positive CAFs and decreased CD8-positive TILs are associated with an immunosuppressive environment in PC, ANO1 may be a key regulatory factor of the TME in PC. A bioinformatics analysis of the TCGA dataset showed the same results. Furthermore, the possible mechanism by which ANO1 affects the TME was investigated, and the results indicated a paracrine mechanism was involved. To the best of

our knowledge, this study is the first to identify the prognostic role of ANO1 and its effect on the TME in PC.

The most specific hallmark of PC is remarkable desmoplasia/fibrosis, which accounts for 80% of the tumors and infiltrating immunosuppressive cells (28). CAFs, including activated pancreatic stellate cells, and their deposition in the extracellular matrix influence tumor progression, metastasis, therapeutic resistance, and angiogenesis (29). CAFs play a key role in tumor promotion through paracrine signaling and direct physical interactions (30). Recent lineage-tracing studies on pancreatic stellate cells have shown that native pancreatic fibroblast populations differ in their ability to expand during carcinogenesis (31, 32). CAFs with opposing functions in PC progression have been identified through single-cell RNA sequencing, multiple immunostaining, and various genetic mouse models (21). myCAFs and iCAFs play the most important functional roles and express FAP and α-SMA, respectively. A previous study showed that depletion of FAP-positive CAFs leads to increase survival rate, while the depletion of α-SMA-positive CAFs, which leads to decrease survival rate (16). PCs tend to have little CD8-positive T cell infiltration but are readily infiltrated by multiple types of immunosuppressive cells, such as FOXP3-
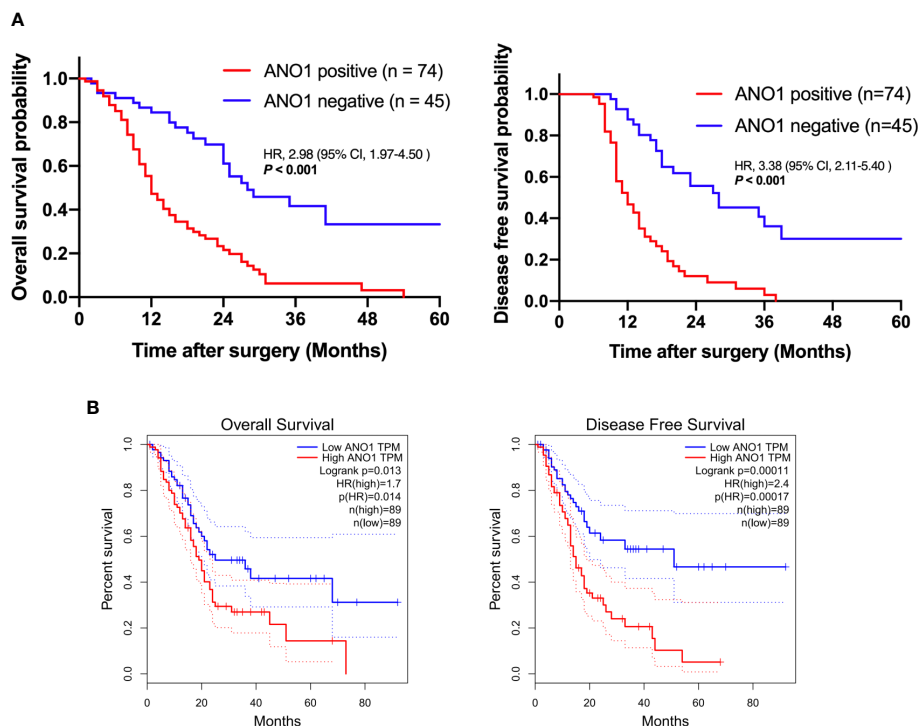
FIGURE 2

Survival analysis based on ANO1 expression. **(A)** Kaplan–Meier curves for overall survival and disease-free survival according to *ANO1* mRNA expression. **(B)** Kaplan–Meier curves for overall survival and disease-free survival according to ANO1 positivity. ANO1, aminooctylamine.

positive Tregs, myeloid suppressor cells, and macrophages (33). previous studies have shown that increased numbers of CD8-positive TILs are associated with better survivalin patients with colorectal and ovarian cancer, whereas an increase in the number of Tregs is linked with poor survival in patients with PC (24, 34). Notably, CAFs have a clear relationship with immune cells. FAP-positive CAFs and α-SMA-positive CAFs can regulate both tumor-related pathways and Treg accumulation. Inhibition of α-SMA-positive CAFs can reduce the Teff/Treg ratio and promote tumor growth (35). Conversely, inhibition of FAP-positive CAFs decreases CD11b-positive myeloid cells and reduces PC growth (20, 36). Previous studies have shown that the general functional contribution of α-SMA-positive CAFs is tumor suppression, which is partly mediated by its production of type I collagen and IL-6 (37). However, this IL-6 production does not promote the progression of

TABLE 2 Univariate and multivariate analysis of overall survival according to ANO1 expression in patients with pancreatic cancer.

Characteristics	Univariate analysis		Multivariate analysis	
	HR	P	HR	
Age >65 years	0.941	0.777		
male	0.692	0.092		
CA19-9 >37 ng/mL	1.530	0.108		
Total bilirubin >1 μmol/L	1.300	0.348		
Tumor size >30 mm	1.202	0.403		
pT3,4	1.004	0.984		
pN1	3.128	0.001	4.073	0.001
Poor Differentiation	0.727	0.142		
Ne1,2,3	0.740	0.163		
Location (head)	1.011	0.958		
ANO1 positivity	3.203	0.001	4.137	0.001

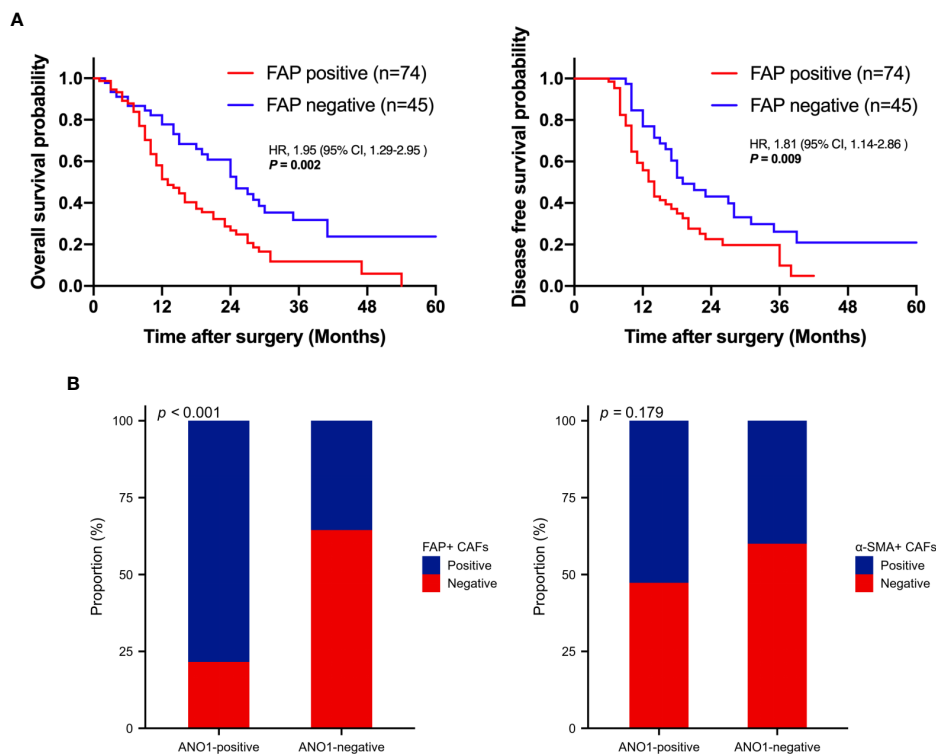ANO1, aminooctylamine; HR, hazard ratio; CA19-9, Carbohydrate antigen-199.

FIGURE 3
Survival analysis based on FAP positivity and correlation analysis between ANO1, FAP, and α-SMA. **(A)** Kaplan–Meier curves for overall survival and disease-free survival according to FAP positivity. **(B)** Correlation analysis between ANO1, FAP, and α-SMA. FAP, fibroblast activation protein; ANO1, aminooctylamine; α-SMA, alpha smooth muscle actin.
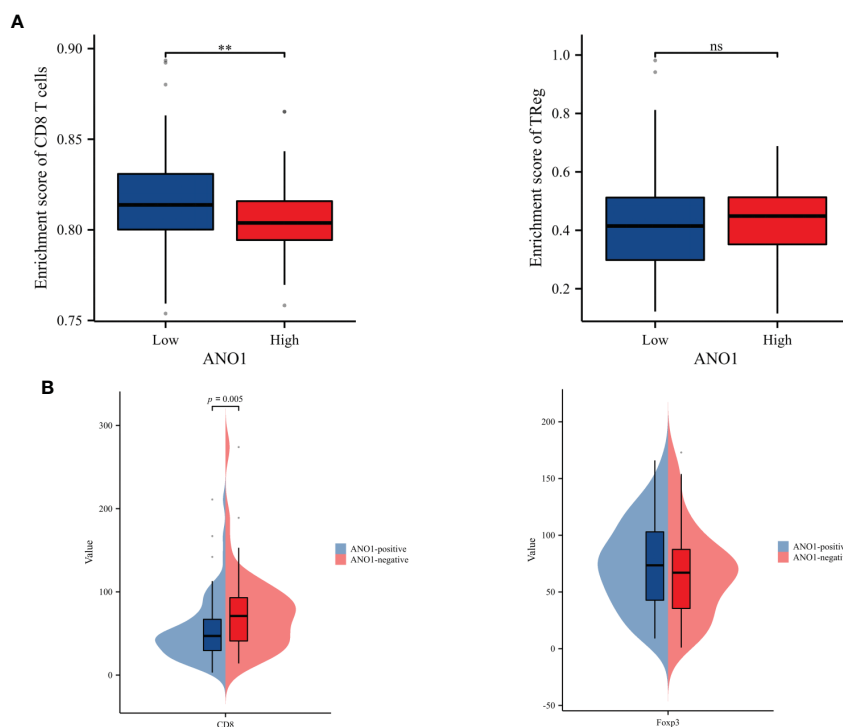

FIGURE 4
Correlation analysis between ANO1 and the numbers of CD8-positive and FOXP3-positive TILs. **(A)** The boxplot of the relationships between ANO1 and CD8 T cells and Tregs by ssGSEA. **(B)** Correlation analysis between ANO1 and the numbers of CD8-positive and FOXP3-positive TILs. ANO1, aminooctylamine; TIL, tumor-infiltrating lymphocyte; FOXP3, forkhead box protein 3; Treg, regulatory T cell; ssGSEA, single sample gene set enrichment analysis; **: $p < 0.01$; ns: not significant.
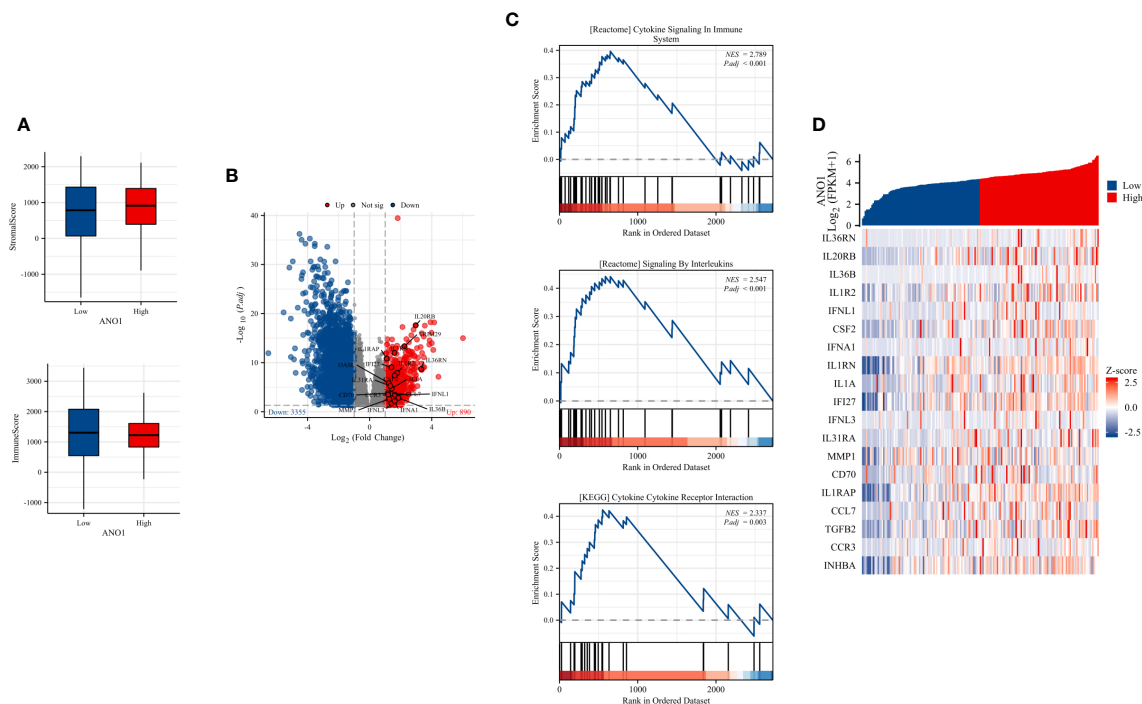
FIGURE 5
ImmuneScore, StromalScore, identiFIcation of DEGs based on ANO1 expression, and GSEA pathway enrichment. **(A)** The boxplot of the StromalScore and ImmuneScore of PC patients based on ANO1 expression. **(B)** The distribution of DEGs in the high and low ANO1 expression groups using volcano plots. **(C)** GSEA pathway enrichment analyses. **(D)** The heatmap of cytokines and receptors in the high and low ANO1 expression groups. DEG, Differential Expression Analysis; ANO1, aminooctylamine; GSEA, gene set enrichment analysis; PC, pancreatic cancer.

PC, and we observed an approximately 50% decrease in IL-6 in the TME (16). FAP-positive CAFs inhibit T cell infiltration into the tumor through CXCL12, and depletion of these fibroblasts or targeting of CXCL12 increases the sensitivity to immune checkpoint blockade of PC in preclinical models (38). Interestingly, although CD4-positive T cell ablation enables CD8-positive T cell-mediated deterioration of pancreatic tumors in mice, consumption of FOXP3-positive Tregs accelerates tumorigenesis as a result of compensatory myeloid infiltration (39). Our study found that ANO1 expression positively correlated with FAP-positive CAFs and negatively correlated with CD8-positive TILs, suggesting that ANO1 may be a key regulator of the tumor immune microenvironment.

Ion channel dysfunction is an emerging field in cancer research, and the differential expression of several types of ion channels in cancer have been reported (15, 26, 40). As a calcium-activated chloride channel, ANO1 can increase vascular smooth muscle contractility and can be a promising target for treating hypertension (41). The expression of ANO1 is influenced by multiple molecular mechanisms (42). Recent studies have revealed that ANO1 expression is controlled by 11q13 gene amplification and that ANO1 may play a cell-specific role through its interconnected protein network, phosphorylation of different kinases, and signaling pathways (11). We found that ANO1 is highly expressed in various malignancies and is associated with poor survival outcomes, which highlight its potential as a biomarker for the detection of certain malignancies. ANO1 not only inhibits tumor apoptosis but also promotes tumor immune escape. Recent researches have revealed that ANO1 overexpression promotes the progression of lung cancer, head and

neck squamous cell carcinoma, and breast cancer through the epidermal growth factor receptor signaling pathway (43, 44). Specifically, in breast cancer cells, ANO1, epidermal growth factor receptor, and signal transducer and transcriptional activator 3 form a positive feedback pathway that promotes cancer cell proliferation and growth (45). ANO1 also activates the Ras-Raf-MEK-ERK1/2 signaling pathway, contributing to the development of head and neck squamous cell carcinoma and colon cancer (45). In esophageal squamous cell carcinoma, ANO1 regulates the tumor growth factor-B signaling pathway and promotes proliferation, migration, and invasion (46). In addition, ANO1 promotes metastasis of liver cancer and ovarian cancer by activating the phosphatidylinositol 3 kinase/protein kinase B signaling pathway (13, 47). However, the relationship between ANO1 and the TME has attracted increasing attention. Research have revealed that ANO1 is participate in immune escape in digestive system-related tumors (48). In one study, ANO1-expressing esophageal squamous cell carcinoma cells activated NFκB signaling in fibroblasts, stimulating CCL1 production, and subsequently enhance invasion (49). In gastrointestinal stromal tumors, the expression of ANO1 was significantly negatively correlated with infiltration of plasma cells and memory-activating CD4-positive T cells, suggesting that ANO1 may be participate in the functional suppression of T cells (50). ANO1 also conduces to immunosuppression of TME and induces acquired resistance to anti-PD-1 immunotherapy, while knockdown or inhibition of ANO1 enhances immunotherapy efficacy and overcomes resistance to immunotherapy. From the mechanism, ANO1 inhibits ferroptosis of cancer in a phosphatidylinositol 3 kinase/protein kinase B signaling-

TABLE 3   Correlation between ANO1 expression and cytokines and their receptors.

Name	Log2FoldChange	P value
IL36RN	3.316874325	2.00614E-09
IL20RB	2.965935052	2.4319E-18
IL36B	1.860432719	0.001536937
IL1R2	1.774740442	1.25503E-08
IFNL1	1.619699413	0.000355941
CSF2	1.614460098	3.973E-08
IFNA1	1.612978271	0.006911448
IL1RN	1.600195515	1.02219E-12
IL1A	1.418821194	1.82205E-05
IFI27	1.400404271	8.84722E-10
IFNL3	1.395986775	0.022168648
IL31RA	1.327320896	5.49237E-06
MMP1	1.255647561	0.002562962
CD70	1.172359866	0.000176168
IL1RAP	1.090599539	1.43772E-11
CCL7	1.354835717	0.000199447
TGFB2	1.260333078	6.35852E-08
CCR3	1.18356959	0.000365243
INHBA	1.087432619	9.39505E-06

dependent manner, promotes tumor progression by promoting tumor growth factor-B release, and promotes the recruitment of CAFs, thereby anti-tumor immunity mediated by CD8-positive T cells is weakened and resistance to immunotherapy is generated (51). However, the role of ANO1 in PC has rarely been investigated. We speculated that ANO1 might regulate the TME through regulating the infiltration of FAP-positive CAFs and CD8-positive TILs in a paracrine manner. Through bioinformatics analysis of the TCGA dataset, we found that ANO1 may regulate the TME of PC through cytokine signaling, interleukin signaling, and cytokine-cytokine receptor interaction signaling pathways; however, the specific mechanisms remain to be further studied.

Our study has certain limitations. First. this was a single-center study, and the sample size limited the validity of our results. Therefore, a larger number of cases and mechanistic studies are required to validate our results. Second, to our knowledge, this is the first research to report that ANO1 is positively associated with CD8-positive TILs and FAP-positive CAFs in PC. However, our analysis used only immunohistochemistry, Therefore, this phenomenon needs to be further confirmed *in vivo* and *in vitro*.

In conclusion, ANO1 is an important prognostic factor for patients with PC after radical resection. ANO1 may induce an immunosuppressive tumor microenvironment in PC cells in a paracrine manner; therefore, ANO1 may be a new therapeutic target in PC.

Data availability statement

The raw data supporting the conclusions of this article will be made available by the authors, without undue reservation.

Ethics statement

The studies involving humans were approved by Institutional Review Committee of the Affiliated Hospital of North Sichuan Medical College (number: 2023ER041-1). The studies were conducted in accordance with the local legislation and institutional requirements. The human samples used in this study were acquired from primarily isolated as part of your previous study for which ethical approval was obtained. Written informed consent for participation was not required from the participants or the participants' legal guardians/next of kin in accordance with the national legislation and institutional requirements.

Author contributions

GZ: Conceptualization, Data curation, Methodology, Writing – original draft. ZS: Data curation, Formal analysis, Methodology, Writing – original draft. JY: Writing – original draft. JL: Writing – original draft. PY: Writing – original draft. BW: Writing – original draft. DD: Writing – original draft. SY: Writing – original draft. YL: Writing – original draft. DR: Writing – original draft. YH: Writing – review & editing. CL: Writing – original draft, Writing – review & editing.

Conflict of interest

The authors declare that the research was conducted in the absence of any commercial or financial relationships that could be construed as a potential conflict of interest.

Publisher's note

All claims expressed in this article are solely those of the authors and do not necessarily represent those of their affiliated organizations, or those of the publisher, the editors and the reviewers. Any product that may be evaluated in this article, or claim that may be made by its manufacturer, is not guaranteed or endorsed by the publisher.

References

1. Rahib L, Smith BD, Aizenberg R, Rosenzweig AB, Fleshman JM, Matrisian LM. Projecting cancer incidence and deaths to 2030: the unexpected burden of thyroid, liver, and pancreas cancers in the United States. *Cancer Res* (2014) 74(11):2913–21. doi: 10.1158/0008-5472.CAN-14-0155

2. Rahib L, Wehner MR, Matrisian LM, Nead KT. Estimated projection of US cancer incidence and death to 2040. *JAMA Netw Open* (2021) 4(4):e214708. doi: 10.1001/jamanetworkopen.2021.4708

3. Kleeff J, Korc M, Apte M, La Vecchia C, Johnson CD, Biankin AV, et al. Pancreatic cancer, Nature reviews. *Dis Primers* (2016) 2:16022. doi: 10.1038/nrdp.2016.22

4. Cronin KA, Scott S, Firth AU, Sung H, Henley SJ, Sherman RL, et al. Annual report to the nation on the status of cancer, part 1: National cancer statistics. *Cancer* (2022) 128(24):4251–84. doi: 10.1002/cncr.34479

5. Groot VP, Rezaee N, Wu W, Cameron JL, Fishman EK, Hruban RH, et al. Patterns, timing, and predictors of recurrence following pancreatectomy for pancreatic ductal adenocarcinoma. *Ann Surg* (2018) 267(5):936–45. doi: 10.1097/SLA.0000000000002234

6. Siegel RL, Miller KD, Jemal A. Cancer statistics, 2020. *CA: Cancer J Clin* (2020) 70(1):7–30. doi: 10.3322/caac.21590

7. Caputo A, Caci E, Ferrera L, Pedemonte N, Barsanti C, Sondo E, et al. TMEM16A, a membrane protein associated with calcium-dependent chloride channel activity. *Sci (New York NY)* (2008) 322(5901):590–4. doi: 10.1126/science.1163518

8. Pedemonte N, Galietta LJ. Structure and function of TMEM16 proteins (anoctamins). *Physiol Rev* (2014) 94(2):419–59. doi: 10.1152/physrev.00039.2011

9. Wang Q, Leo MD, Narayanan D, Kuruvilla KP, Jaggar JH. Local coupling of TRPC6 to ANO1/TMEM16A channels in smooth muscle cells amplifies vasoconstriction in cerebral arteries, American journal of physiology. *Cell Physiol* (2016) 310(11):C1001–9. doi: 10.1152/ajpcell.00092.2016

10. Ji Q, Guo S, Wang X, Pang C, Zhan Y, Chen Y, et al. Recent advances in TMEM16A: Structure, function, and disease. *J Cell Physiol* (2019) 234(6):7856–73. doi: 10.1002/jcp.27865

11. Duvvuri U, Shiwarski DJ, Xiao D, Bertrand C, Huang X, Edinger RS, et al. TMEM16A induces MAPK and contributes directly to tumorigenesis and cancer progression. *Cancer Res* (2012) 72(13):3270–81. doi: 10.1158/0008-5472.CAN-12-0475-T

12. Britschgi A, Bill A, Brinkhaus H, Rothwell C, Clay I, Duss S, et al. Calcium-activated chloride channel ANO1 promotes breast cancer progression by activating EGFR and CAMK signaling. *Proc Natl Acad Sci U States America* (2013) 110(11):E1026–34. doi: 10.1073/pnas.1217072110

13. Zhang C, Liu J, Han Z, Cui X, Peng D, Xing Y. Inhibition of TMEM16A suppresses growth and induces apoptosis in hepatocellular carcinoma. *Int J Clin Oncol* (2020) 25(6):1145–54. doi: 10.1007/s10147-020-01653-6

14. Deng L, Yang J, Chen H, Ma B, Pan K, Su C, et al. Knockdown of TMEM16A suppressed MAPK and inhibited cell proliferation and migration in hepatocellular carcinoma. *OncoTargets Ther* (2016) 9:325–33. doi: 10.2147/OTT.S95985

15. Sauter DRP, Novak I, Pedersen SF, Larsen EH, Hoffmann EK. ANO1 (TMEM16A) in pancreatic ductal adenocarcinoma (PDAC). *Pflugers Archiv: Eur J Physiol* (2015) 467(7):1495–508. doi: 10.1007/s00424-014-1598-8

16. Biffi G, Oni TE, Spielman B, Hao Y, Elyada E, Park Y, et al. IL1-induced JAK/STAT signaling is antagonized by TGFβ to shape CAF heterogeneity in pancreatic ductal adenocarcinoma. *Cancer Discovery* (2019) 9(2):282–301. doi: 10.1158/2159-8290.CD-18-0710

17. Lo A, Li CP, Buza EL, Blomberg R, Govindaraju P, Avery D, et al. Fibroblast activation protein augments progression and metastasis of pancreatic ductal adenocarcinoma. *JCI Insight* (2017) 2(19). doi: 10.1172/jci.insight.92232

18. Kraman M, Bambrough PJ, Arnold JN, Roberts EW, Magiera L, Jones JO, et al. Suppression of antitumor immunity by stromal cells expressing fibroblast activation protein-alpha. *Sci (New York NY)* (2010) 330(6005):827–30. doi: 10.1126/science.1195300

19. Santos AM, Jung J, Aziz N, Kissil JL, Puré E. Targeting fibroblast activation protein inhibits tumor stromagenesis and growth in mice. *J Clin Invest* (2009) 119(12):3613–25. doi: 10.1172/JCI38988

20. Özdemir BC, Pentcheva-Hoang T, Carstens JL, Zheng X, Wu CC, Simpson TR, et al. Depletion of carcinoma-associated fibroblasts and fibrosis induces immunosuppression and accelerates pancreas cancer with reduced survival. *Cancer Cell* (2014) 25(6):719–34. doi: 10.1016/j.ccr.2014.04.005

21. McAndrews KM, Chen Y, Darpolor JK, Zheng X, Yang S, Carstens JL, et al. Identification of functional heterogeneity of carcinoma-associated fibroblasts with distinct IL6-mediated therapy resistance in pancreatic cancer. *Cancer Discovery* (2022) 12(6):1580–97. doi: 10.1158/2159-8290.CD-20-1484

22. Wang LC, Lo A, Scholler J, Sun J, Majumdar RS, Kapoor V, et al. Targeting fibroblast activation protein in tumor stroma with chimeric antigen receptor T cells can inhibit tumor growth and augment host immunity without severe toxicity. *Cancer Immunol Res* (2014) 2(2):154–66. doi: 10.1158/2326-6066.CIR-13-0027

23. Ma C, Dong X. Colorectal cancer-derived Foxp3(+) IL-17(+) T cells suppress tumour-specific CD8+ T cells. *Scand J Immunol* (2011) 74(1):47–51. doi: 10.1111/j.1365-3083.2011.02539.x

24. Naito Y, Saito K, Shiiba K, Ohuchi A, Saigenji K, Nagura H, et al. CD8+ T cells infiltrated within cancer cell nests as a prognostic factor in human colorectal cancer. *Cancer Res* (1998) 58(16):3491–4.

25. Bose T, Cieślar-Pobuda A, Wiechec E. Role of ion channels in regulating Ca^{2+} homeostasis during the interplay between immune and cancer cells. *Cell Death Dis* (2015) 6(2):e1648. doi: 10.1038/cddis.2015.23

26. Pardo LA, Stühmer W. The roles of K(+) channels in cancer, Nature reviews. *Cancer* (2014) 14(1):39–48. doi: 10.1038/nrc3635

27. Pedersen SF, Hoffmann EK, Novak I. Cell volume regulation in epithelial physiology and cancer. *Front Physiol* (2013) 4:233. doi: 10.3389/fphys.2013.00233

28. Halbrook CJ, Lyssiotis CA, Pasca di Magliano M, Maitra A. Pancreatic cancer: Advances and challenges. *Cell* (2023) 186(8):1729–54. doi: 10.1016/j.cell.2023.02.014

29. Velez-Delgado A, Donahue KL, Brown KL, Du W, Irizarry-Negron V, Menjivar RE, et al. Extrinsic KRAS signaling shapes the pancreatic microenvironment through fibroblast reprogramming. *Cell Mol Gastroenterol Hepatol* (2022) 13(6):1673–99. doi: 10.1016/j.jcmgh.2022.02.016

30. LeBleu VS, Kalluri R. A peek into cancer-associated fibroblasts: origins, functions and translational impact. *Dis Models Mech* (2018) 11(4). doi: 10.1242/dmm.029447

31. Garcia PE, Adoumie M, Kim EC, Zhang Y, Scales MK, El-Tawil YS, et al. Differential contribution of pancreatic fibroblast subsets to the pancreatic cancer stroma. *Cell Mol Gastroenterol Hepatol* (2020) 10(3):581–99. doi: 10.1016/j.jcmgh.2020.05.004

32. Huang H, Wang Z, Zhang Y, Pradhan RN, Ganguly D, Chandra R, et al. Mesothelial cell-derived antigen-presenting cancer-associated fibroblasts induce expansion of regulatory T cells in pancreatic cancer. *Cancer Cell* (2022) 40(6):656–673.e7. doi: 10.1016/j.ccell.2022.04.011

33. Daley D, Zambirinis CP, Seifert L, Akkad N, Mohan N, Werba G, et al. γδ T cells support pancreatic oncogenesis by restraining αβ T cell activation. *Cell* (2016) 166(6):1485–1499.e15. doi: 10.1016/j.cell.2016.07.046

34. Teng F, Mu D, Meng X, Kong L, Zhu H, Liu S, et al. Tumor infiltrating lymphocytes (TILs) before and after neoadjuvant chemoradiotherapy and its clinical utility for rectal cancer. *Am J Cancer Res* (2015) 5(6):2064–74.

35. Nolz JC. Molecular mechanisms of CD8(+) T cell trafficking and localization. *Cell Mol Life Sci: CMLS* (2015) 72(13):2461–73. doi: 10.1007/s00018-015-1835-0

36. Rhim AD, Oberstein PE, Thomas DH, Mirek ET, Palermo CF, Sastra SA, et al. Stromal elements act to restrain, rather than support, pancreatic ductal adenocarcinoma. *Cancer Cell* (2014) 25(6):735–47. doi: 10.1016/j.ccr.2014.04.021

37. Chen Y, Kim J, Yang S, Wang H, Wu CJ, Sugimoto H, et al. Type I collagen deletion in αSMA(+) myofibroblasts augments immune suppression and accelerates progression of pancreatic cancer. *Cancer Cell* (2021) 39(4):548–565.e6. doi: 10.1016/j.ccell.2021.02.007

38. Feig C, Jones JO, Kraman M, Wells RJ, Deonarine A, Chan DS, et al. Targeting CXCL12 from FAP-expressing carcinoma-associated fibroblasts synergizes with anti-PD-L1 immunotherapy in pancreatic cancer. *Proc Natl Acad Sci U States America* (2013) 110(50):20212–7. doi: 10.1073/pnas.1320318110

39. Zhang Y, Lazarus J, Steele NG, Yan W, Lee HJ, Nwosu ZC, et al. Regulatory T-cell depletion alters the tumor microenvironment and accelerates pancreatic carcinogenesis. *Cancer Discovery* (2020) 10(3):422–39. doi: 10.1158/2159-8290.CD-19-0958

40. Pedersen SF, Stock C. Ion channels and transporters in cancer: pathophysiology, regulation, and clinical potential. *Cancer Res* (2013) 73(6):1658–61. doi: 10.1158/0008-5472.CAN-12-4188

41. Heinze C, Seniuk A, Sokolov MV, Huebner AK, Klementowicz AE, Szijártó IA, et al. Disruption of vascular Ca2+-activated chloride currents lowers blood pressure. *J Clin Invest* (2014) 124(2):675–86. doi: 10.1172/JCI70025

42. Guo S, Zhang L, Li N. ANO1: more than just calcium-activated chloride channel in cancer. *Front Oncol* (2022) 12:922838. doi: 10.3389/fonc.2022.922838

43. Wang H, Yao F, Luo S, Ma K, Liu M, Bai L, et al. A mutual activation loop between the Ca(2+)-activated chloride channel TMEM16A and EGFR/STAT3 signaling promotes breast cancer tumorigenesis. *Cancer Lett* (2019) 455:48–59. doi: 10.1016/j.canlet.2019.04.027

44. Bill A, Alex Gaither L. The mechanistic role of the calcium-activated chloride channel ANO1 in tumor growth and signaling. *Adv Exp Med Biol* (2017) 966:1–14. doi: 10.1007/5584_2016_201

45. Sui Y, Sun M, Wu F, Yang L, Di W, Zhang G, et al. Inhibition of TMEM16A expression suppresses growth and invasion in human colorectal cancer cells. *PloS One* (2014) 9(12):e115443. doi: 10.1371/journal.pone.0115443

46. Yu Y, Cao J, Wu W, Zhu Q, Tang Y, Zhu C, et al. Genome-wide copy number variation analysis identified ANO1 as a novel oncogene and prognostic biomarker in esophageal squamous cell cancer. *Carcinogenesis* (2019) 40(10):1198–208. doi: 10.1093/carcin/bgz077

47. Liu Z, Zhang S, Hou F, Zhang C, Gao J, Wang K. Inhibition of Ca(2+) -activated chloride channel ANO1 suppresses ovarian cancer through inactivating PI3K/Akt signaling. *Int J Cancer* (2019) 144(9):2215–26. doi: 10.1002/ijc.31887

48. Gasparotto D, Sbaraglia M, Rossi S, Baldazzi D, Brenca M, Mondello A, et al. Tumor genotype, location, and Malignant potential shape the immunogenicity of primary untreated gastrointestinal stromal tumors. *JCI Insight* (2020) 5(22). doi: 10.1172/jci.insight.142560

49. Pinto MC, Schreiber R, Lerias J, Ousingsawat J, Duarte A, Amaral M, et al. Regulation of TMEM16A by CK2 and its role in cellular proliferation. *Cells* (2020) 9(5). doi: 10.3390/cells9051138

50. Li Q, Zhi X, Zhou J, Tao R, Zhang J, Chen P, et al. Circulating tumor cells as a prognostic and predictive marker in gastrointestinal stromal tumors: a prospective study. *Oncotarget* (2016) 7(24):36645–54. doi: 10.18632/oncotarget.9128

51. Jiang F, Jia K, Chen Y, Ji C, Chong X, Li Z, et al. ANO1-mediated inhibition of cancer ferroptosis confers immunotherapeutic resistance through recruiting cancer-associated fibroblasts. *Adv Sci (Weinheim Baden-Wurttemberg Germany)* (2023) 10 (24):e2300881. doi: 10.1002/advs.202300881